

Protoneutron star dynamos and pulsar magnetism

A. Bonanno^{1,2}, V. Urpin^{3,4}, and G. Belvedere¹

¹ INAF, Osservatorio Astrofisico di Catania, Via S.Sofia 78, 95123, Catania, Italy

² INFN, Sezione di Catania, Via S.Sofia 72, 95123, Catania, Italy

³ A.F. Ioffe Institute of Physics and Technology, St. Petersburg, Russia

⁴ Isaac Newton Institute of Chile, Branch in St. Petersburg, 194021 St. Petersburg, Russia

September 18, 2018

Abstract. We have investigated the turbulent mean-field dynamo action in protoneutron stars that are subject to convective and neutron finger instabilities during the early evolutionary phase. While the first one develops mostly in the inner regions of the star, the second one is favored in the outer regions, where the Rossby number is much smaller and a mean-field dynamo action is more efficient. By solving the mean-field induction equation we have computed the critical spin period below which no dynamo action is possible and found it to be ~ 1 s for a wide range of stellar models and for both axisymmetric and non-axisymmetric magnetic fields. Because this critical period is substantially longer than the characteristic spin period of very young pulsars, we expect that a mean-field dynamo will be effective for most protoneutron stars. The saturation dipole field estimated by making use of the model of “global” quenching fits well the pulsar magnetic fields inferred from the spin-down data. Apart from the large scale magnetic field, our model predicts also a generation of small scale fields which are typically stronger than the poloidal field and can survive during the lifetime of pulsars. Extremely rapidly rotating protoneutron stars ($P \sim 1$ ms) may have the dipole field $\sim (3 - 6) \times 10^{14}$ G.

Key words. MHD - pulsars: general - stars: neutron - magnetic fields

1. Introduction

The origin of pulsar magnetism is a subject of debate for decades. In a simple magnetic dipole braking model, the polar field strength inferred from observational data can reach $\sim 5 \times 10^{13}$ G. One possibility is that the magnetic field of a progenitor star is amplified by many orders of magnitude because of the conservation of the magnetic flux during the collapse stage (Ginzburg 1964, Woltier 1964). However, the “fossil field” hypothesis despite being seemingly attractive and plausible meets a number of problems. For instance, the progenitor star should possess a sufficiently strong magnetic field that does not agree with observational data (see discussion in Thompson & Duncan 1993 for more details).

Another possibility is a turbulent dynamo action that can amplify the magnetic field during first $\sim 30 - 40$ s of a neutron star life when the star is the subject of hydrodynamic instabilities. Hydrodynamic instabilities in protoneutron stars (PNSs) are driven by either lepton gradients which result in the so-called “neutron-finger instability” (Bruenn & Dineva 1996), or by negative entropy gradients which are common in simulations of supernovae (Bruenn & Mezzacappa 1994, Rampp & Janka 2000) and in models of PNSs (Keil & Janka 1995; Keil, Janka & Müller 1996; Pons et al. 1999). The latter instability

is usually referred to as the “convective instability”. The nature of instabilities in PNSs has been considered by a number of authors (Grossman, Narayan & Arnett 1993, Bruenn & Dineva 1996, Miralles, Pons & Urpin 2000). Turbulent motions caused by instabilities in combination with rapid rotation that seems to be almost unavoidable in PNSs make turbulent dynamo one of the most plausible mechanism responsible for the pulsar magnetism.

Recent measurements of X-ray spectra of some pulsars have started to provide a closer look at the magnetic field at the neutron star surface. These observations indicate that the pulsar magnetic field may often have a fine structure near the surface apart from the global magnetic structure inferred from the spin-down data. For instance, the absorption features in the spectrum of 1E 1207.4-5209 allow to estimate a surface magnetic field as $\sim 1.5 \times 10^{14}$ G (Sanwal et al. 2002), that is in contrast with the dipolar magnetic field estimated from the spin-down rate of this pulsar ($\sim (2 - 4) \times 10^{12}$ G (Pavlov et al. 2002)). Becker et al. (2003) have found an emission line in the X-ray spectrum of PSR B1821-24 that could be interpreted as cyclotron emission from the pulsar’s polar cap. The line can be formed in a magnetic field $\sim 3 \times 10^{11}$ G, approximately two orders of magnitude stronger than the dipolar magnetic field. Kargaltsev, Pavlov & Romani (2004) have reported a marginal detection of the emission line in the spectrum of the millisec-

ond pulsar J0437-4715 that can be interpreted as a cyclotron line from the magnetic spot with the field $\sim 7 \times 10^8 \text{G}$ on the neutron star surface. Haberl et al. (2003) found evidence for a proton cyclotron line in the spectrum of the isolated pulsar RBS 1223. This line corresponds to the local magnetic field at the stellar surface of approximately one order of magnitude stronger than the dipole field. All these measurements provide evidence that the magnetic field likely has a complex structure in neutron stars with small scale fields being stronger than (or comparable to) the large scale field responsible for the secular spin-down of pulsars.

Observations of radio emitting pulsars also support the idea that neutron stars apart from the large scale field (likely, dipoles) may have small scale magnetic structures at the surface. Recently, Gil & Mitra (2001) and Gil & Melikidze (2002) have argued that the formation of a vacuum gap in radio pulsars is possible if the magnetic field lines near the polar cap have a small curvature $\sim 10^5 \text{cm}$ and the field is very strong, $B_s \sim 10^{13} \text{G}$, irrespective of the magnetic field measured from the spin evolution. Furthermore, the presence of a strong magnetic field with a small curvature can account for the radio emission of many radiopulsars that lie in the pulsar graveyard and should be radio silent (Gil & Mitra 2001). Analysing drifting subpulses observed in many pulsars, Gil & Sendyk (2003) found that their behavior is consistent with the vacuum gap maintained by a strong spot-like magnetic field.

The growing number of evidences for a complex structure of the magnetic field suggests that this may represent a general phenomenon in neutron stars. The presence of a large scale field accompanied by small scale magnetic structures can naturally be understood if the field is generated by the turbulent mean-field dynamo. The duration of an unstable stage in PNSs ($\sim 30 - 40 \text{s}$) is sufficient for dynamo to reach a saturation level because the period of rotation of PNSs and the dynamo growth time are typically much shorter (Thompson & Duncan 1993). The magnetic fields generated by turbulent dynamo in convective PNSs will be frozen in the crust that starts to form almost immediately after convection stops. Since the crustal conductivity is high both the large and relatively small scale fields can survive in neutron stars during a long time comparable to the lifetime of pulsars (Urpin & Gil 2004).

Recently, it has been shown by Bonanno, Rezzolla & Urpin (2003) that turbulence can drive both small and large scale dynamos in PNSs. This result is in contrast to the previous conclusion by Thompson & Duncan (1993) that only small scale dynamo can be operative in neutron stars. The reasoning of these authors was based on the assumption that the whole PNS is convectively unstable with turbulent velocity $v_T \sim 10^8 \text{cm s}^{-1}$. An efficiency of the mean-field dynamo can be characterized by the Rossby number, $Ro = P/\tau_T$, where P is the period of rotation and τ_T is the turnover time of turbulence. If $P \sim 10 - 100 \text{ms}$ that is likely typical for young neutron stars (Narayan 1987) and $\tau_T \sim 1 \text{ms}$ that is typical for the convectively unstable region of PNSs then $Ro \sim 10 - 100$ and the influence of rotation on the turbulence is therefore weak. As a consequence, Duncan & Thompson (1992) and Thompson & Duncan (1993) concluded that the mean-field dynamo does not operate in PNSs except those rotating with the period $\sim 1 \text{ms}$.

The model of pulsar magnetism qualitatively similar to that by Thompson & Duncan (1993) has been outlined by Wheeler et al. (2000) and Wheeler, Meier & Wilson (2002) who pointed out the importance of differential rotation that seems to be almost unavoidable in PNSs. Their model suggests that a very strong toroidal magnetic field can be generated by differential rotation in a newly born pulsar. These authors assume that a poloidal field of $\sim 10^{12} \text{G}$ could arise simply from flux-freezing if the precollapse progenitor core has a field strength comparable to that of a magnetized white dwarf, $\sim 10^8 \text{G}$. Mention that this point seems to be in contradiction with observational data and has been criticized by Thompson & Duncan (1993). The poloidal field can be amplified further by differential rotation to produce a strong toroidal field. The toroidal field is growing linearly with time, and the growth is limited by buoyancy which operates to expel the field from the site where it is generated. According to the authors, the toroidal field at the buoyancy limit can be as strong as $\sim 10^{16} \text{G}$. Generally, such a strong field can be sufficient to suppress convection in proto-neutron stars (Miralles, Pons & Urpin 2002). Note, however, that the turbulent magnetic diffusion caused by convection can essentially decrease the saturation toroidal field as it will be seen from our calculations and, most likely, the generated field will not suppress convective motions.

In fact, the picture is more complex since two essentially different instabilities may occur in PNSs (Bruenn & Dineva 1996, Miralles, Pons & Urpin 2000). Convection is presumably connected to the entropy gradient, whereas the neutron-finger instability is more relevant to a negative lepton gradient. The neutron-finger instability is the astrophysical analogy of the salt fingers that exist in terrestrial oceans. Physically, a fluid parcel perturbed downward in the PNS can thermally equilibrate more rapidly with the background but find itself lepton-poorer and denser and, therefore, subject to a downward force that would amplify perturbations. The neutron-finger instability is a sort of the so called “doubly diffusive” instabilities that occur due to dissipative processes like viscosity, thermal and lepton diffusivity. These processes are rather fast in PNSs and, therefore, the secular neutron-finger instability can grow rapidly. The estimated growth time in the neutron-finger unstable region, $\sim 30 - 100 \text{ms}$, is only a couple orders of magnitude longer than the growth time of extremely rapid convection (Miralles, Pons, & Urpin 2000), thus yielding a mean turbulent velocity $\sim (1 - 3) \times 10^6 \text{cm/s}$.

Typically, the convectively unstable region is surrounded by the neutron-finger unstable region, the latter involving therefore a larger portion of the stellar material. As a result, not the whole PNS is convectively unstable in contrast to the assumption made by Thompson & Duncan (1993). Instabilities first develop in the outer layers containing $\sim 30\%$ of the stellar mass, The two unstable regions move towards the inner parts of the star and, after $\sim 10 \text{s}$, more than 90% of the stellar mass is hydrodynamically unstable. At this stage the stellar core has become convectively unstable but it is still surrounded by an extended neutron-finger unstable region. In $\sim 20 \text{s}$ that follow, the temperature and lepton gradients are progressively reduced and the two unstable regions begin to shrink, leaving the outer regions of the star. After $\sim 30 \text{s}$, most of the PNS is stable and

the instabilities disappear completely after ~ 40 s (Miralles, Pons & Urpin, 2000). The Rossby number is actually large in the convectively unstable region, $Ro \sim 10-100$, and the mean-field dynamo likely does not work in this region. However, this is not the case in the neutron finger unstable region where the turbulent velocity is much slower than in the convectively unstable region, and $Ro \sim 1$ (Bonanno, Rezzolla & Urpin, 2003). Therefore, turbulence can be strongly modified by rotation in the neutron finger unstable region, and this favors the efficiency of a mean-field dynamo. Of course, in both regions turbulent magnetic fields can also be generated by small scale dynamo.

In the present paper, we consider the mean-field dynamo action in PNSs in more detail. We extend our study to the case of non-axisymmetric fields that are of particular interest in pulsars. The main goal of this paper is to show that the mean-field dynamo can operate in a wide range of the parameters of PNSs and generate the field of the strength comparable to that of “standard” pulsars. The paper is organized as follows. In Section 2, we consider the basic equations governing the mean-field dynamo and discuss the properties of convection in PNSs. The numerical results are represented in Section 3, and our findings are summarized in Section 4.

2. Basic equations

To investigate the efficiency of a mean-field dynamo action, we model the PNS as a sphere of radius R with two substantially different turbulent zones separated at $R_c < R$. The inner part ($r < R_c$) corresponds to the convectively unstable region, while the outer one ($R_c < r < R$) to the neutron-finger unstable region. The boundary between the two regions moves inward on a timescale comparable to the cooling timescale (i.e. $\sim 1-10$ s) that is much longer than the turnover time for the both unstable zones. The energy of turbulence is generally non-stationary as well, developing rapidly soon after the collapse, reaching a quasi-stationary regime after a few seconds, and then progressively disappearing. However, changes take place on the cooling time scale and, therefore, all parameters of turbulence can be treated in quasi-steady approximation. In this case, the mean-field induction equation for a turbulent PNS can be written as

$$\frac{\partial \mathbf{B}}{\partial t} = \nabla \times (\mathbf{v} \times \mathbf{B} + \alpha \mathbf{B}) - \nabla \times (\eta \nabla \times \mathbf{B}), \quad (1)$$

where η is the turbulent magnetic diffusivity, α is a pseudo-scalar measuring the efficiency of the dynamo (the “ α -parameter”), and \mathbf{v} is the velocity of a mean fluid motion. Boundary conditions for the magnetic field need to be specified at the stellar surface, where we impose vacuum boundary conditions, and at the center of the star, where we impose the vanishing of the toroidal magnetic field.

We assume that differential rotation is the only large scale motion in PNSs, and $\mathbf{v} = \boldsymbol{\Omega}(r) \times \mathbf{r}$. From theoretical modeling and simple analytic considerations it is commonly accepted that core collapse of a rotating progenitor leads to differential rotation of a newly born neutron star (Zwinger & Müller 1997; Rampp, Müller & Ruffert 1998; Dimmelmeier, Font & Müller 2002) mainly due to conservation of the angular momentum

during collapse. A recent study on evolutionary sequences of rotating PNSs (Villain et al. 2004) shows that the typical scale on which the angular velocity changes is in the range $\approx 5-10$ km. We consider two possible models of differential rotation in PNSs, a shellular rotation with

$$\Omega(r) = \Omega_{sph}^{(0)} + \left(\frac{r}{R}\right)^2 \Omega_{sph}^{(1)}, \quad (2)$$

and cylindrical rotation with

$$\Omega(s) = \Omega_{cyl}^{(0)} + \left(\frac{s}{R}\right)^2 \Omega_{cyl}^{(1)}, \quad (3)$$

where r and s are the spherical and cylindrical radii, respectively. Note that $\Omega(r)$ can generally depend on the time because the PNS cools down and characteristics of turbulence change during the unstable stage. Turbulent transport of the angular momentum takes place on the diffusive timescale, $\sim R^2/v_T^2\tau_T$, that is short compared to the cooling time of PNSs. Therefore, differential rotation is likely constrained to the properties of turbulent motions at each instant of time, and $\Omega(r)$ follows adiabatically the PNS thermal and chemical evolution. We will neglect these relatively slow changes in our quasi-steady modeling. This can well be justified because the main conclusions of our study are qualitatively the same for any considered rotation law including rigid rotation.

As it was mentioned, all of the PNS undergoes turbulent motions but with properties that are different in the inner parts ($0 \leq r \leq R_c$), where fast convection operates, from those in the outer parts ($R_c \leq r \leq R$), where the neutron-finger instability operates. To model this in a simple way, we assume the relevant physical properties of the two regions to vary in a smooth way mostly across a thin layer of thickness $\Delta R = 0.025R$. More precisely, we express η as

$$\eta = \eta_c + (\eta_{nf} - \eta_c) \{1 + erf[(r - R_c)/\Delta R]\} / 2, \quad (4)$$

where η_c and η_{nf} are respectively the turbulent magnetic diffusivities in the convective and neutron-finger unstable zones, and erf is the “error function”. Using equation (4), we have $\eta \approx \eta_c$ if $R_c - r \gg \Delta R$ (convective zone), while $\eta \approx \eta_{nf}$ if $r - R_c \gg \Delta R$ (neutron finger unstable zone). In the both unstable zones, the turbulent magnetic diffusivity can be estimated as $v_T \ell_T / 3$ where v_T and ℓ_T are the corresponding turbulent velocity and length-scale. The turbulent length-scales are likely comparable in the both zones and $\sim 1-3$ km. The turbulent velocities are, however, different with much larger velocity in the convective zone (see Bonanno, Rezzolla & Urpin 2003). Therefore, $\eta_{nf} \ll \eta_c$ in PNSs, and we choose $\eta_{nf}/\eta_c = 0.1$ in calculations.

Similarly, we have modeled the α -parameter as being negligibly small in the convectively unstable region and equal to α_{nf} in the neutron-finger unstable region, i.e.

$$\alpha(r, \theta) = \alpha_{nf} \cos \theta \{1 + erf[(r - R_c)/\Delta R]\} / 2, \quad (5)$$

where the angular dependence chosen in this expression is the simplest guaranteeing antisymmetry across the equator. Usually, we assume $\alpha_{nf} = \text{const}$ in calculations. However, the α_{nf} -parameter is likely not constant in the neutron finger unstable region because differential rotation or inhomogeneity of

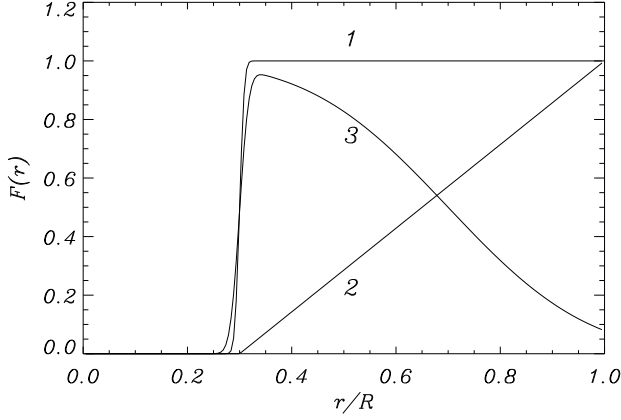


Fig. 1. The sketch of the radial dependence of $F(r)$ for the three models used in our calculations.

turbulence can generally produce some non-uniformity in α . For instance, a non-uniformity can originate from overshooting caused by convection that smooths the boundary layer between the zones. To understand how much our conclusions are sensitive to the choice of α , we performed some calculations with a radially dependent $\alpha_{nf}(r) = \alpha_{nf0}F(r)$ where $F(r)$ is plotted in Fig. 1.

We recall that in a rotating turbulence with length-scale ℓ_T and moderate Rossby number, $\alpha_{nf0} \approx \Omega \ell_T^2 \nabla \ln(\rho v_T^2)$ (Rüdiger & Kitchatinov 1993). In PNSs, however, the pressure is mainly determined by number density of degenerate neutrons and, therefore, the density length-scale is comparable to the pressure one L and to the maximal length-scale of the instabilities. This introduces a great simplification since we have then $\alpha_{nf0} \approx \Omega L$.

3. Numerical results

The induction equation (1) with Ω , η and α given by equations (2)-(3), (4) and (5) has been solved with a numerical code employing finite-difference techniques for the radial dependence and a polynomial expansion for the angular dependence. In particular, we use the representation (Rädler, 1973)

$$\mathbf{B} = \mathbf{B}_p + \mathbf{B}_t, \quad \mathbf{B}_p = \nabla \times \mathbf{A}_t \quad (6)$$

with

$$\mathbf{B}_t = -\mathbf{r} \times \nabla \Psi, \quad \mathbf{A}_t = -\mathbf{r} \times \nabla \Phi \quad (7)$$

and the scalar functions Ψ and Φ have the following expansion

$$\begin{aligned} \Phi &= \sum_{n=1}^{\infty} \sum_{m=-n}^n e^{-i\lambda_{mn}t} \Phi_{nm}(r) Y_n^m(\theta, \phi) \\ \Psi &= \sum_{n=1}^{\infty} \sum_{m=-n}^n e^{-i\lambda_{mn}t} \Psi_{nm}(r) Y_n^m(\theta, \phi) \end{aligned} \quad (8)$$

The induction equation thus decouple in a $m \times n$ -dependent set of coupled equations for Ψ and Φ which can be solved by truncating the order n of the harmonics for a given value of m (further details can be found in Rädler, 1973, Bonanno *et al*, 2002).

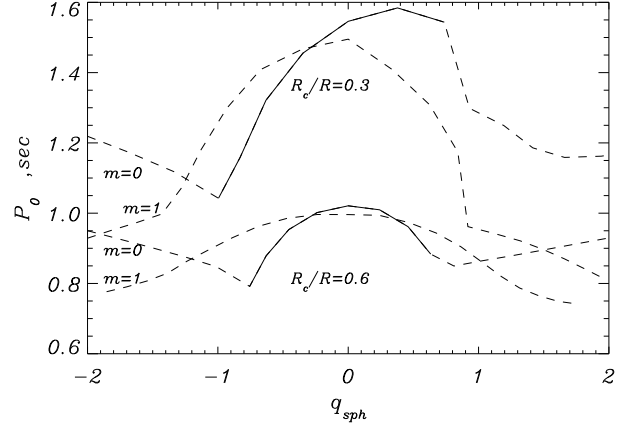


Fig. 2. Critical period as a function of the differential rotation parameter q_{sph} for $F(r) = 1$. The two pairs of curves refer to different values of R_c , with the solid parts corresponding to a stationary dynamo and the dashed parts to an oscillatory dynamo. The number m corresponds to different values of the azimuthal wavenumber in a polynomial expansion for the magnetic field.

Non axisymmetric modes, *i.e.* those with $m \neq 0$ are waves traveling in azimuthal direction. The field configuration of a non-axisymmetric mode rotates like a rigid body with angular velocity λ_{mn}/m . The simulations reported here use 30 spherical harmonics and about 40 grid points in the radial direction in order to ensure convergence. Boundary conditions are chosen in order to guarantee the regularity at the center and vacuum outside $r = R$. We have solved the induction equation (1) to determine the critical value α_0 corresponding to the marginal stability of the dynamo. The seed magnetic field will grow if $\alpha_{nf0} > \alpha_0$ and decay if $\alpha_{nf0} < \alpha_0$. Since $\alpha_{nf0} \approx \Omega L$, the critical value α_0 effectively selects a critical value for the spin period, $P_0 \equiv 2\pi L/\alpha_0$, such that magnetic field generation via a mean-field dynamo action will be possible only if the stellar spin period is shorter than the critical one. The different types of dynamo can be distinguished according to whether the generated field exhibits periodic oscillations (oscillatory dynamo, dashed lines in Fig.2) or not (stationary dynamo, solid lines)

In Fig.2, we plot the critical period P_0 for the case of the shellular rotation (2). The critical period is shown as a function of the parameter $q_{sph} = \Omega_{sph}^{(1)}/(\Omega_{sph}^{(0)} + \Omega_{sph}^{(1)})$ that characterizes differential rotation. Note that $q > 0$ and $q < 0$ correspond to situations in which the stellar surface rotates faster and slower than the center, respectively. Calculations have been done for $\eta_{nf} = 10^{11} \text{ cm}^2 \text{ s}^{-1}$ and $F(r) = 1$ (constant α -parameter in the neutron finger unstable region). The different types of dynamo can be distinguished according to whether the generated field exhibits periodic oscillations (oscillatory dynamo, dashed lines in Fig.2) or not (stationary dynamo, solid lines).

As shown in Fig.2, a stationary dynamo dominates the axisymmetric magnetic field generation process for $|q| \lesssim 1$, while an oscillatory dynamo is more efficient for $1 \lesssim |q|$. These two regimes correspond to α^2 -dynamo and $\alpha\Omega$ -dynamo, respec-

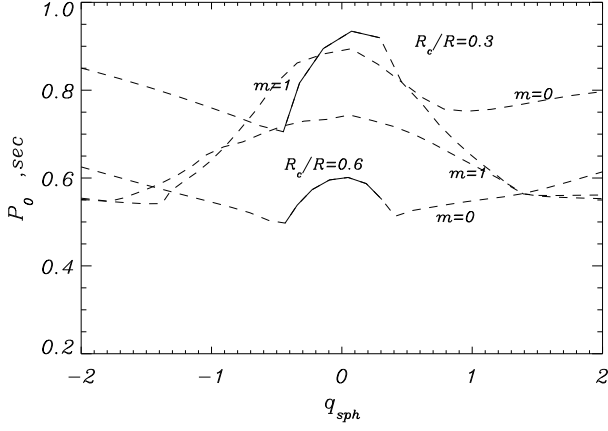


Fig. 3. Critical period as a function of the differential rotation parameter q_{sph} for $F(r)$ given by the model 2 in Fig.1. Other parameters are the same as in Fig.2.

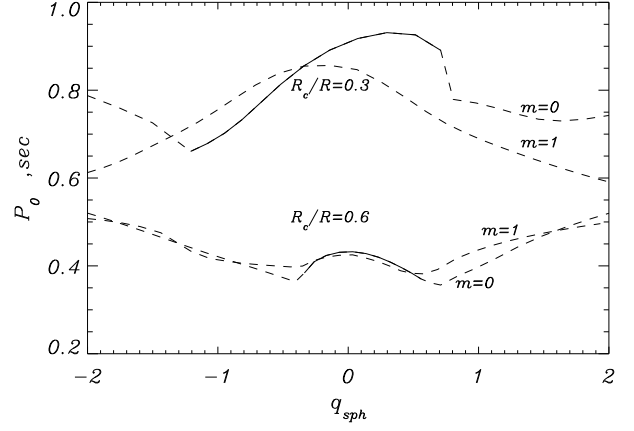


Fig. 4. Critical period as a function of the differential rotation parameter q_{sph} for $F(r)$ given by the model 3 in Fig.1. Other parameters are the same as in Figs.2 and 3.

tively. Given the large differential rotation required for a generation of the axisymmetric oscillatory magnetic field, it may be difficult to achieve in practice. Hence, the α^2 -dynamo appears to be the most likely source of axisymmetric magnetic field generation via dynamo processes in PNSs. The situation is, however, different for the generation of a non-axisymmetric magnetic field that is of interest for PNSs since the observed pulsars have non-axisymmetric fields.

The critical spin period found in our calculations is in general rather long. For instance, a mean-field dynamo will develop if $P \leq 1$ s when $R_c/R = 0.6$ and if $P \leq 1.4$ s when $R_c/R = 0.3$ if a PNS rotates rigidly (i.e. $q_{sph} = 0$). If the PNS rotates differentially, the critical period is typically reduced. The difference, however, is not large except the case of the non-axisymmetric field ($m = 1$) in a star with $|q_{sph}| > 1$ when the difference can reach $\sim 40\%$. As a result, only PNSs with $P \gtrsim 1$ s will not be subject to a turbulent mean-field dynamo action. Such slow rotation rates should be rather difficult to achieve if angular momentum is conserved during the collapse to a PNS. We expect, therefore, that a turbulent mean-field dynamo will be effective during the initial stages of the life of most PNSs.

In Fig.(3) and (4), we plot the same as in Fig.(2) but for $F(r)$ represented by the lines 2 and 3 in Fig.(1), respectively. The behavior of P_0 is qualitatively unchanged and the only difference is that there is no stationary dynamo regime for a generation of the axisymmetric field in the case $R_c/R = 0.6$ if the function $F(r)$ is decreasing to the surface (the model 3 in Fig.(1)). Like the case $F(r) = 1$, the critical period is longer for $R_c/R = 0.3$ compared to $R_c/R = 0.6$. The difference is due to the fact that a PNS with a more extended neutron-finger unstable region can rotate proportionally more slowly while maintaining the same dynamo action. The values of P_0 are typically by a factor ~ 2 smaller than for a dynamo action with $F(r) = 1$ implying that the onset of dynamo is mainly characterized by the average value of α in the unstable region rather than a particular dependence of α on r .

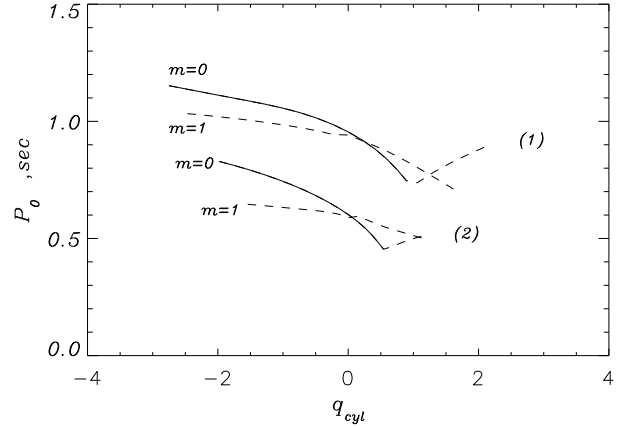


Fig. 5. Critical period as a function of the differential rotation parameter q_{cyl} for $F(r)$ given by the models (1) and (2) in Fig.1. for $R_c/R = 0.6$.

The above discussion for the shellular model Eq.(2), remains qualitatively similar for a cylindrical rotational law Eq.(3) for $q_{cyl} = \Omega_{cyl}^{(1)}/(\Omega_{cyl}^{(0)} + \Omega_{cyl}^{(1)})$. Since in this case the differential rotation is not important the basic dynamo action is that of an α^2 -model. If instead $q_{cyl} \gtrsim 1$, the dynamo mechanism would produce an oscillating field of an $\alpha\Omega$ -type. The general dependence of the critical period on the differential rotation parameter q_{cyl} is shown in Fig.(5) for $R_c = 0.6R$. Note that, for small q_{cyl} , the $m = 1$ modes have a greater critical periods than the $m = 0$ modes, and thus the critical value of α_{nf0} for non-axisymmetric modes is smaller than for the axisymmetric case. As a consequence, non-axisymmetric field is more easily excited than the axisymmetric one in this case.

In Fig.(6), we show the toroidal (B_ϕ) and poloidal (B_p) magnetic fields of a typical PNS model for the cylindrical rotation law. Note that the both components are generated in the outer neutron-finger unstable region but turbulent diffusion

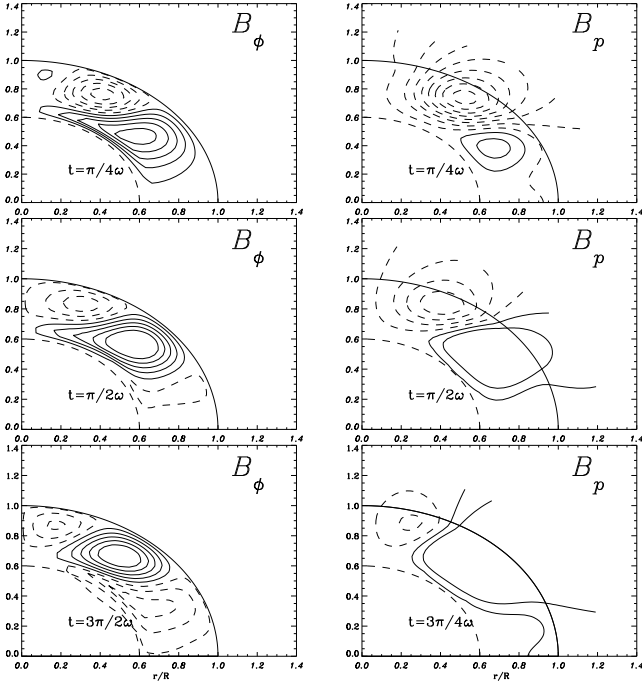


Fig. 6. Toroidal (B_ϕ) and the poloidal (B_p) magnetic field lines for different pulsational times for $m = 0$ and $q \approx 2$ in Fig.(5). Solid and dashed contours correspond to positive and negative values, respectively. The dot-dashed line marks the position of $R_c = 0.6R$.

transports the magnetic field also in the inner convectively unstable region. This field is, however, considerably weaker. Our calculations show that if $|q| < 1$ and the field is generated by the α^2 -dynamo then $B_\phi/B_p \sim 10$, while $B_\phi/B_p \sim 100 - 200$ if $|q| > 1$ and the $\alpha\Omega$ -dynamo generates the magnetic field. Both results suggest that the internal magnetic fields in neutron stars could be substantially stronger than the observable surface fields. The toroidal magnetic field tends to concentrate near the polar regions whereas the poloidal one is more evenly distributed in latitude. Note that, in the case of an α^2 -dynamo, the generated field propagates more efficiently into the convective zone (see Bonanno, Rezzolla and Urpin 2003),

4. Discussion

The PNS is subject to two substantially different instabilities, with a convective instability operating in the inner region of the star and a neutron-finger instability being more efficient in the outer region. The turbulent motions are more rapid in the convective zone, where the Rossby number is large but the α -parameter, characterizing the mean-field dynamo action, is likely small. In the neutron-finger unstable region, on the other hand, the turbulent turnover time is considerably longer, the Rossby number small, and the α -parameter can be sufficiently large to drive a mean-field dynamo.

The α -parameter depends the stellar rotation being larger for rapidly rotating stars. Our simulations show that even relatively slowly rotating PNSs can be subject to a dynamo action, with the α^2 -dynamo being the most efficient mechanism

of generation for both axisymmetric and non-axisymmetric fields if differential rotation is not extremely strong. The calculated critical value of the spin period that determines the onset of dynamo in PNSs is $P_0 \sim 1$ s for a wide range of models. This value is essentially larger even than the characteristic spin period of very young pulsars as inferred from observations ($\sim 50 - 100$ ms, Narayan 1987) but likely PNSs can rotate even faster. As a result, a turbulent mean-field dynamo can be effective in the early stages of the life of most PNSs. The critical period is not very different for axisymmetric and non-axisymmetric fields and likely both these magnetic configurations can be generated by the PNS dynamo. The generation of a non-axisymmetric component is the key point for the magnetism of pulsars since they have a substantial non-axisymmetric field. It must be stressed that, as the neutron-finger unstable region shrinks towards the surface, the difference between axisymmetric and non-axisymmetric critical periods, disappears as it can be noticed, for instance, in Fig. 2 and Fig. 3 thus providing an opportunity to generate a non-axisymmetric field in a very general framework.

The PNS dynamo can operate both in oscillatory and stationary regime. A non-axisymmetric field is always a wave traveling in the azimuthal direction. On the other hand, axisymmetric field can develop in both the oscillatory and stationary regimes, depending on the profile of α in the neutron finger unstable region and the thickness of this region. The period of dynamo oscillations can be estimated as $\sim 0.1R^2/\eta_{mf} \sim R^2/\eta_c$ and, in our model, is ~ 1 s. Note that, for the pulsar magnetism, there is no particular difference in which regime, oscillatory or stationary, the field is generated because a formation of the crust starts almost immediately after the instability stops, and the generated field should be frozen-in a highly conductive crustal matter.

The unstable stage lasts $\sim 30 - 40$ s in PNSs, and likely this time is sufficient for the dynamo to reach a saturation level. We estimate the field strength in saturation by making use of the model of a “global” quenching. In accordance with this model, a generation of the magnetic field decreases the α -parameter, and the simplest possible expression can be proposed for the non-linear α -parameter in the neutron finger unstable zone,

$$\alpha_{nl}(\tilde{B}) = \frac{\alpha_{nf0}}{1 + \tilde{B}^2/B_{eq}^2}, \quad (9)$$

where \tilde{B} is the characteristic value of the generated field, and B_{eq} is the equipartition magnetic field determined by equating the kinetic and magnetic energy of turbulence. Then, the saturation magnetic field, B_{sat} , can be estimated if we assume that $\alpha_{nl}(B_{sat})$ is equal to the critical value α_0 that determines the marginal dynamo stability. We have from this condition

$$B_{sat} \approx B_{eq} \sqrt{\frac{P_0}{P} - 1}, \quad (10)$$

If $P_0 > P > P_0/2$, the generated mean field is weaker than the turbulent magnetic field, B_{eq} . On the contrary, the saturation field is stronger than B_{eq} if $P < P_0/2$, and B_{sat} can reach a rather large value if the PNS rotates very rapidly. Likely, however, that the rotation period cannot be shorter than ~ 1 ms

and, hence, the maximum field generated by dynamo in PNSs is around $\sim 30B_{eq}$. In our calculations, the generated toroidal field is typically stronger than the poloidal field. Therefore, quenching is determined mostly by the strength of the toroidal field, and equation (10) provides an estimate of the saturation toroidal field. Since, in the case of an α^2 -dynamo, the poloidal field is approximately 5-10 times weaker, we obtain for the saturation poloidal field

$$B_{p\ sat} \approx (0.1 - 0.2)B_{eq} \sqrt{\frac{P_0}{P} - 1}. \quad (11)$$

The poloidal field is typically weaker than (or comparable to) the equipartition field. The only exception is very rapidly rotating PNSs with the period $\sim 1 - 3$ ms where the poloidal field can be a factor few stronger than small-scale turbulent fields. In the majority of pulsars, however, we can expect that a large scale poloidal (for example, dipolar) field should not be stronger than the small-scale fields if their magnetism is caused by the mean-field dynamo action. Note that because of a high conductivity, turbulent magnetic fields with the length-scale $\gtrsim 1$ km can survive in the neutron star crust for a very long time comparable to the lifetime of pulsars, ~ 100 Myr (Urpin & Gil 2004).

Turbulence is non-stationary in the both unstable zones of PNSs, and therefore B_{eq} in equation (9)-(11) varies with time. It rises very rapidly soon after collapse, reaches some quasi-steady regime, and then goes down when the temperature and lepton gradients are smoothed (after $\sim 30 - 40$ s). The timescale required for fluid to make one turn in a turbulent cell with the length-scale ℓ_T can be estimated as $\tau_T \approx \pi \ell_T / v_T$. This timescale varies with time as well, but is typically much shorter than the characteristic cooling timescale of the PNS, τ_{cool} , except the very late phase when gradients are smoothed and instabilities are less efficient. Therefore, turbulence can be treated in a quasi-steady approximation during almost the whole convective evolution of the PNS except the late stage. We can estimate B_{eq} during the quasi-steady regime as $\sim 10^{16}$ G in the convective zone, and $\sim (1 - 3) \times 10^{14}$ G in the neutron finger unstable zone (see Urpin & Gil 2004). However, the temperature and lepton number gradients are progressively reduced as the PNS star cools down and, therefore, the turbulent velocity decreases as well. As a result, the strength of small-scale magnetic fields generated by turbulence also decreases compared to the maximum value, but the turnover time of turbulence increases. The mean-field dynamo as well as the small-scale one are still operative until the quasi-steady condition $\tau_{cool} \gg \tau_T$, is fulfilled. We assume that this condition breaks down at some instant of time when τ_T becomes comparable to the cooling timescale: $\tau_T \sim \tau_{cool}$. Then, the turbulent velocity at this instant is given by

$$v_T \sim \frac{\pi \ell_T}{\tau_{cool}}. \quad (12)$$

We assume that the final strength of the magnetic field generated by both the mean-field and small-scale dynamo is determined by B_{eq} at the instant of time when the quasi-steady con-

dition breaks down. Therefore, we have for the final strength of the equipartition magnetic field

$$B_{eq} \sim \sqrt{4\pi\rho v_T} \sim \frac{\pi\sqrt{4\pi\rho\ell_T}}{\tau_{cool}}. \quad (13)$$

The final strength of the generated small-scale field turns out to be the same for both unstable zones. For the largest turbulent scale, $\ell_T = L \sim 1 - 3$ km, estimate (13) yields $B_{eq} \sim 3 \times 10^{13}$ G if τ_{cool} is of the order of a few seconds. Using this estimate of B_{eq} , we can conclude that the strength of a large-scale poloidal field generated by the mean-field dynamo (equation (8)) is in a good agreement with the observed magnetic fields of the majority of pulsars. For example, the generated poloidal field is $\sim (1 - 2) \times 10^{13}$ G if the star rotates with the period ~ 100 ms. Note that extremely rapidly rotating PNSs ($P \sim 1$ ms) may possess a very strong poloidal field $\sim (3 - 6) \times 10^{14}$ G comparable to that of magnetars.

Acknowledgements. VU thanks INFN (Catania) and Dipartimento di Fisica ad Astronomia, University of Catania, for financial support. AB thanks L.Rezzolla for important comments on the manuscript.

References

- Becker W., Swartz D., Pavlov G., Elsner D., Grindlay J., Mignani R., Tennant A., Backer D., Pulone L., Testa V., Weisskopf M. 2003, ApJ, 594, 798
- Bonanno A., Elstner D., Rüdiger G., Belvedere G. 2002. A&A, 390, 673
- Bonanno A., Rezzolla L., Urpin V. 2003. A&A, 410, L33
- Bruenn S., Dineva T. 1996, ApJ, 458, L71
- Bruenn S., Mezzacappa A. 1994, ApJ, 433, L45
- Dimmelmeier H., Font J. A., Müller E. 2002, A&A, 393, 523
- Duncan R., Thompson C. 1992. ApJ, 392, L9
- Gil J., Melikidze G. 2002, ApJ, 577, 909
- Gil J., Mitra D. 2001. ApJ, 550, 383
- Gil J., Sendyk M. 2003. ApJ, 585, 453
- Ginzburg V. 1964. Dokl. Akad. Nauk SSSR, 156, 43
- Grossman S., Narayan R., Arnett D. 1993. ApJ, 407, 284
- Haberl F., Schwöpe A., Hambaryan V., Hasinger G., Motch C. 2003. A&A, 403, 19
- Kargaltsev O., Pavlov G., Romani R. 2004. ApJ, 602, 327
- Keil W., Janka H.-T. 1995, A&A, 296, 145
- Keil W., Janka H.-T., Müllerr E. 1996, ApJ, 473, L111
- Miralles J., Pons J., Urpin V. 2000, ApJ, 543, 1001
- Miralles J., Pons J., Urpin V. 2002, ApJ, 574, 356
- Narayan R. 1987, ApJ, 319, 162
- Pavlov G., Zavlin V., Sanwal D., Trümper J. 2002, ApJ, 569, L95
- Pons J., Reddy S., Prakash M., Lattimer J., Miralles J. 1999, ApJ, 513, 780
- Rampp M., Janka H.-T. 2000, ApJ, 539, L33
- Rampp M., Müller E., Ruffert M. 1998, A&A, 332, 969
- Rädler K.-H., Astron. Nachr. Bd. 294, (1973)
- Rüdiger G., Kitchatinov L. 1993. A&A, 269, 581
- Sanwal D., Pavlov G., Zavlin V., Teter M. 2002, ApJ, 574, L61
- Thompson C., Duncan R. 1993, ApJ, 408, 194
- Urpin V., Gil J. 2004. A&A, 415, 305
- Villain L., Pons J., Cerdá-Durán P.,ourgoulhon E. 2004. A&A, 418, 283
- Wheeler J.C., Yi I., Höflich P., Wang L. 2000. ApJ, 537, 810
- Wheeler J.C., Meier D., Wilson J.R. 2002. ApJ, 568, 807
- Woltjer L. 1964. ApJ, 140, 1309
- Zwergner T., Müller E. 1997, A&A, 320, 209